Fracture and Failure Behaviour of Jute Fabric Reinforced Polypropylene. Effect of Interface Modification

B.A. Acha [a], J. Karger-Kocsis [a*] and M. M. Reboredo [b]

[a] Institut für Verbundwerkstoffe GmbH (Institute for Composite Materials), Kaiserslautern University of Technology, D-67663 Kaiserslautern, Germany

[b] Institute of Materials Science and Technology (INTEMA), University of Mar del Plata - National Research Council (CONICET), Av. Juan B. Justo 4302, 7600, Mar del Plata. Argentina.

* Corresponding author.
Email address: karger@ivw.uni-kl.de

Submitted to Polymer and Polymer Composites, April and revised June 2005.

ABSTRACT

The tensile fracture and failure behaviour of jute cloth (25 wt.%) reinforced polypropylene (PP) composites were studied as a function of certain interface modification procedures. The latter covered esterification of the jute and the use of lignin and maleated PP (PPMAN) as modifiers. The tensile and fracture mechanical characteristics of the composites were determined. Analysis of the emitted acoustic signals along with fractographic inspection served to trace the failure and damage development. The best property improvement was achieved by using PPMAN. The observed notch-sensitivity for the specimens was attributed to missing reinforcement homogeneity owing to the presence of insufficient jute cloth layers.

KEYWORDS: polypropylene composite, jute cloth, fracture, failure, acoustic emission, fracture mechanics.

1. INTRODUCTION

Polypropylene (PP), one of the most "popular" thermoplastic polymers, has the advantages of low cost, easy recyclability, and relatively high thermal stability. Thus PP often serves as the matrix in composites. Among the reinforcements used, increasing attention has been recently paid to natural fibres[1-6]. The growing interest for natural fibres is mainly due to their economical production, low cost, biodegradability and environmental benefits ("zero CO_2 emission"). These fibres have low specific gravity, high specific strength and stiffness,[7] suffer little damage during processing and they are less abrasive than mineral fillers in their action on the mould and mixing/compounding equipment. Among the natural fibres, jute appears to be a promising candidate as reinforcement for PP composites.[8] It has been already proved as a satisfactory reinforcement for thermoset composites[9]. Jute fibres are relatively tough and have a high aspect ratio in comparison with other natural fibres.[4] Jute clothes, woven fabrics (sacks) are widely used, however, they are still only used a little for polymer reinforcement[8]. Because of the lack of adhesion between hydrophilic cellulose fibres and hydrophobic PP, the resulting composites possess unsatisfactory properties.

It is well known that the mechanical performance of composites depends not only on the properties of the individual components, but also on their interfacial bonding. The interface/interphase plays a crucial role in determining the properties of fibre-reinforced materials. [10,11] To improve the compatibility, either PP should be made more hydrophilic, or the cellulosic reinforcements more hydrophobic, or both[12,13]. For example, Clemons et al.[14] found that the wetting of maleic anhydride (MAN) esterified aspen fibres by the PP matrix was much better that that of the untreated version. Mishra and Naik[15], who esterified several lignocellulosic fibres with MAN and used them to prepare composites

with polystyrene as matrix, found that this treatment reduced the moisture absorption of both the fibres and their resulting composites, with respect to the untreated systems.

On the other hand, one of the usual polymeric coupling agents, that behaves most effectively in PP/natural fibres composites is maleic anhydride grafted polypropylene (PPMAN). Felix and Gatenholm[2] studied the wetting of MAN-esterified cellulose fibres with PP and PPMAN and observed more effective wetting of the fibres by using PPMAN. Further, many researchers demonstrated that this grafted polymer improved the interfacial adhesion between cellulosic fibres and PP matrix and yielded improved composite properties.[16-19]

Attempts were also made to utilize lignin as a compatibilizer in various polymer systems.[20,21] Since lignin contains[22] polar (hydroxyl) groups and non-polar hydrocarbon and benzene rings, it was presumed that lignin was also a useful compatibilizer for PP/cellulosic composites.

This work was devoted to study the fracture and failure behaviour of woven jute reinforced PP composites as a function of interface modification. The latter was achieved by esterification of the jute and by incorporation of compatibilizers, PPMAN and lignin.

2. EXPERIMENTAL

2.1 Materials

Commercial bidirectional jute fabrics (plain weave 0/90; with the same amount of roving in the weft and warp directions) were used as the reinforcement layers. The volumetric and surface densities of the fabrics were 0.464 ± 0.05 g/cm^3 and 0.027 ± 0.002 g/cm^2, respectively. The fibre linear density of the jute (which is a measure of the average number of fibres in the cross section of a given yarn) was 310 ± 60 tex.

The mechanical parameters of the jute fibres were determined in accordance with ASTM D3379-75 (single filament tensile test). To calculate these parameters, an average fibre diameter of 66 μm ± 16, (taken as the average measured diameter of 300 specimens), was used. The average ultimate strength of the untreated jute (σ_f) was 407.42 ± 148.68 MPa and the average tangent modulus of elasticity was 19.26 ± 4.61 GPa.

Jute fibres were esterified in order to improve their compatibility with the PP matrix, using a commercial alkenyl succinic anhydride (ASA, Lasar 2019 CE, Akzo Nobel). The fabrics were dried at 70°C in a vacuum oven until a constant weight was reached. The esterification reactions were carried out by immersing the jute fabric in a solution of acetone containing 96 g/l of ASA and a catalyst (4-dimethyaminopyridine, Fluka, concentration: 8.75 g/l) and then heating at reflux temperature (56.5 °C) for 4 hours. The esterified jute fabric was removed from the acetone solution and intensively washed with distilled water in order to eliminate the unreacted materials. Finally, it was dried at 70°C in a vacuum oven.

A polypropylene (PP) homopolymer, (melt flow index:11 g/min at 230°C and 2.16 kg load) provided by Petroquimica Cuyo, was used as matrix. As compatibilizer a commercial PPMAN (Epolene G3003 from Eastman Kodak and Lignin (Curan 2711 P) supplied by Lignotech (Sweden) served in this work.

2.2 Composite production

PP with 5 wt.% of compatibilizer was blended in a heated intensive mixer at 180ºC for 10 min and then pelletized. The pellets were then compression moulded using a hydraulic press at 180ºC and 7.4 MPa to prepare films of ca.1mm thickness. In this case, the blends were allowed to melt for 10 min and then pressure was applied for another 10 min.

Composites were produced by the film stacking technique, i.e. layers of jute fabric were sandwiched between the PP films. The samples were compression moulded at 180ºC and 7.4 MPa for 25 min. The jute fabric was dried in a vacuum oven at 70ºC overnight prior to hot pressing.

Four different types of composite were prepared:

a) Neat PP with 25 wt.%. of jute cloth (PPJ).

b) Neat PP with 25 wt.% of esterified jute cloth (PPJLa).

c) PP modified by 5wt.% of Epolene G3003 and reinforced with 25% wt. of jute (PPGJ).

d) PP modified by 5wt.% of Lignin and reinforced with 25% wt. of jute (PPLJ).

The composite sheets contained three layers of jute cloth resulted in 25 wt.% nominal reinforcement content.

2.3 Testing

Static tensile tests were performed on dumbbells cut from the plates. The width of these dumbbells was 20 mm instead of the usual 10 mm (type 1B, DIN EN ISO 527-2 standard). This width allows us to determine reliable tensile values as the damage zone size in such composites may reach 15-20 mm.[23] This test was carried out at room temperature and 1 mm/min crosshead speed. At least five specimens of each composite were tested to obtain the average mechanical properties. Rectangular strips (1 and 3 layers) cut from the jute cloth were also subjected to tensile loading. In order to get information about the failure mode, the acoustic emission (AE) activity was registered using one microphone during loading of the specimens.

To trace the damage development, static mechanical tests were also performed on single edge-notched tensile loaded (SEN-T) specimens. Their dimensions allowed the location of the acoustic emission (AE) via a four sensors array (Figure 1). Tensile loading of the SEN-

T specimens (two specimens of each composite were tested) occurred at room temperature at a deformation rate of 1 mm/min on a Zwick 1474 machine. The notch (a_0) was initially sawn and then sharpened by razor blade tapping. The fracture toughness values were determined by the formulae cited in refs. 24 and 25, considering the maximum load (K_Q) and the 5% offset value (K_C), respectively.

The damage zone was estimated by location of the acoustic emission (AE) events, collected during loading of the SEN-T specimens. The AE activity was recorded in-situ by a Defektophone NEZ 220 device (AEKI, Budapest, Hungary).

Wide bandwidth (100-600 kHz) microsensors (Micro 30D of Physical Acoustic Co., Princeton, USA) were used as AE sensors. Location occurred by a built-in algorithm of the device in the knowledge of the acoustic wave speed. To estimate the size of the damage zone, a mathematical weighting procedure, described elsewhere [26, 27], was used. Briefly, the located map was scanned by a circle of 6 mm diameter in 1 mm steps in both X and Y directions (Figure 1). The percentage of the located events within the circle was considered for each surface point in the z-direction, resulting in two- or three-dimensional contour plots. The damage zone was assigned to the surface that contained 90% of all the located AE events.

2.4 Morphological observations

The fracture surfaces of the specimens from tensile testing were sputter- coated with gold and observed by using a JEOL -6400 scanning electron microscope (SEM, Tokyo, Japan).

3. RESULTS AND DISCUSSION

3.1 Tensile fracture and failure

Figure 2 shows the apparent stress-strain (σ_{app} vs. ε) curves for the jute cloth. One can clearly recognize the "strain-hardening" behaviour of the jute cloth. This suggests that the "mesh" size of the cloth was very large (in fact ca. 1 x 1 mm) and the jute threads within can well be stretched. Note that multiplication of the jute layers did result in multiplied stress values.

Characteristic stress-strain curves for the composites are depicted in Figure 3. The highest ductility (highest ε value) was that of the PPJ composite. We believe that this was due to poor bonding between the jute and the PP. This, which was also reflected in a low modulus value, should favour stress relief and redistribution in the damage zone leading at the end to high strain values. Poor bonding between the jute cloth and PP should be accompanied by satellite cracking and a long pull-out length of jute. The highest stiffness and strength at low elongations were delivered by the PPGJ composite, in which the bonding between the jute and the PP was markedly better (Table 1). The surprising fact that the strength values of PPJ and PPGJ were similar can be explained by a combined strain- hardening effect of the jute and PP, which is allowed by the weak interface between them.

Some information on the interface effect can be deduced from the cumulative AE events versus elongation curves. The later the AE starts, and the steeper its course, the better the interfacial bonding is, and thus the higher the stiffness and strength values are. [28]

Changes in the slope of the ΣAE event curves, such as the appearance of a shoulder (Figure 4), imply satellite cracking. They appeared perpendicular to the loading (Figure 5) which is usual even for advanced composites containing fibres oriented perpendicularly to the loading direction.

It is worth noting that the changes in the slope of the curve of ΣAE versus ε were more prominent when they were normalized in respect with the ultimate failure (ε_{max}).

Further details are suggested by considering the AE amplitude distribution data. Attention should be paid to the fact that no AE occurred in section I of the σ-ε curves. AE activity was registered only in sections II and III (Figure 6 a). The AE amplitude histograms from section II were very similar for PPJ, PPJL and PPJLa. That is why Figure 6b depicts only PPJ. This suggests that neither the incorporation of lignin nor the jute esterification were very successful in improving the interface between PP and jute.

The fact that the AE activity and AE amplitude distribution were very similar for PPJ and jute cloth (cf. Figure 6b) indicates that jute cloth was the AE source and the related events were less influenced by the interface or bulk PP. This is an indirect indication of the poor adhesion between jute and PP. On the other hand the number of AE events and the amplitude distribution of PPGJ differed for those of PPJ and jute (Figure 6b). The amplitude distribution histograms of PPGJ showed two peaks instead of a monotonously descending feature. Recall that macroscopically less satellite matrix cracks were observed for PPGJ than for PPJ, PPJL and PPJLa. So the peak at ca. 30 dB could be assigned to fibre/matrix debonding, whereas the other one at ca. 40 dB was attributed to pull-out events following the jute fracture. This speculation is based on the usual AE amplitude ranking, i.e. matrix-related events< fibre/matrix debonding< fibre pull-out< fibre fracture events.

Unfortunately clustering of the AE amplitudes and their assignment to given individual failure events cannot be done without in-situ observation (and AE assessment) of the corresponding failure. Nevertheless, the macrophotograph in Figure 7 clearly demonstrates the difference in the interface debonding between PPJ and PPGJ. The latter failed by brittle matrix cracking, along with limited pull-out of the jute fibres. On the other hand PPJ fractured with multiple ductile matrix cracking, associated with extensive pull-out. Recall that the more prominent the pull-out, the worse the interface bonding is.

3.2 Damage development

Figure 8 shows the force as a function of displacement for the composite SEN-T specimens. The curves in Figure 8 show a different ranking for the modification compared to the tensile response. Obviously, notching has a great influence on the fracture behaviour. The major reason should be the jute cloth reinforcement. Its mesh size could be too large, and the three layers incorporated do not guarantee the necessary reinforcement "homogenization". [23, 29]

Figure 8 suggests that PPJ and PPJLa fractured in a brittle way, whereas the PPGJ and especially PPLJ did so in a ductile manner. The damage zones determined up to maximum load are depicted in Figure 9. To a first approximation, the smaller the damage zone, the better the interface bonding. Furthermore, good bonding is associated with the centre of the damage zone being close to the initial notch (indicated in Figure 9). It is clear that the latter requirement is not met. So, the crack had propagated already at the maximum load. Therefore the K_Q values cannot represent the initiation values (Table 2). A further remark for good interface bonding is that the number of AE events is low. By considering the AE-related damage zone the interfacial bonding quality is PPJLa>PPGJ>PPJ>PPLJ. Recall that this ranking does not agree with that of the tensile test results. This result should be related to the "reinforcement homogenization", the lack of which produces "notch sensitivity". Notch sensitivity means that the failure mode may change on notching because stress transfer in the notch tip is affected by the (locally) very inhomogeneously distributed jute cloth. Figures 10 and 11 show fractographic inspection of the fractured SEN-T specimens. Both PPJ and PPJLa failed by brittle matrix cracking. On the other hand, PPGJ and PPLJ showed ductile matrix failure (Figure 11).

The reason for the ductile matrix failure of PPGJ and PPLJ is different. It was due to good bonding ensuring effective stress transfer from the matrix to the jute fibres in PPGJ. In contrast, the lignin particles, acting as stress concentrations and causing cavitation in the PP, were responsible for the ductile failure of the matrix in PPLJ. In Figure 12 the lignin particles are well resolved on the fracture surface. This SEM picture demonstrates that the lignin works as a modifier for the bulk matrix instead of the interface.

4. CONCLUSIONS

The mechanical response of the composites depends on the interface/bulk modification. In addition, notching of the specimens may change their fracture and failure behaviour fundamentally. This notch sensitivity was attributed to a lack of "reinforcement homogenization" (a few jute cloth layers having too high a mesh size).

Monitoring the acoustic emission (AE) proved to be a suitable tool to detect changes in the failure mode and the damage development caused by interface modifications. The course of the cumulative AE events and cover curve of the AE amplitude distributions can deliver useful information on the adhesion between the matrix and jute.

ACKNOWLEDGMENTS

B. A. Acha thanks the DAAD (German Academic Exchange Service) for her fellowship at the Institut für Verbundwerkstoffe GmbH (IVW).

References

1. Bataille P., Ricard L. and Sapieha S., Polymer Composites, 10, (1989), 103.

2. Felix J. M. and Gatenholm P., Journal of Applied Polymer Science, 42, (1991), 609.

3. Aranberri-Askargorta I., Lampke T. and Bismarck A., Journal of Colloid and Interface Science, (2003), 580.

4. Chen X., Guo Q. and Mi Y., Journal of Applied Polymer Science, 69, (1998), 1891.

5. Fung K. L., Li R. K. Y and Tjongs S. C., Journal of Applied Polymer Science, 85, (2002), 169.

6. López Manchado M. A., Arroyo M., Biagiotti L. and Kenny J. M., Journal of Applied Polymer Science, 90, (2003), 2170.

7. George J., Sreekala M. S. and Thomas S., Polymer Engineering and Science, 41, (2001), 1471.

8. Munikenche Gowda T., Naidu A.C.B. and Chaja R., Composites Part A, 30, (1999),

277.

9. Mohanty A. K and Misra M., Polymer Plastics Technology and Engineering, 34, (1995),

729.

10. Harris B., Beaumont P. W. R. and Moncunill de Ferran E., Journal of Materials Science, 6, (1971), 238.

11. Sanadi A. R., Subramanion R. V. and Manoranjan V. S., Polymer Composites, 12, (1991), 377.

12. Gauthier R., Joly C., Coupas A. C., Gauthier H. And Escoubes M., Polymer Composites, 19, (1998), 287.

13. Nuñez A. J., Kenny J. M., Reboredo M. M., Aranguren M. I., and Marcovich N.E., Polymer Engineering and Science, 42, (2002), 733.

14. Clemons C., Young R. A. and Rowell R. M., Wood and Fibre Science, 24, (1992), 353.

15. Mishra S. and Naik J. B., Journal of Applied Polymer Science., 68, (1998),681.

16. Avella M., Casale L., Dell'Erba R., Focher B., Martuscelli E. and Marzetti A. J., Journal of Applied Polymer Science, 68, (1998),1077.

17. Kazayawoko M., Balatinecz J. J. and Matuana L.M, Journal of Materials Science, 34, (1999), 6189.

18. Gassan J. and Bledzki A. K., Composites: Part A, 28, (1997). 1001.

19. Ichazo M. N., Albano C., González J., Perera R. and Candal M. V., Composite Structures, 54, (2001), 207.

20. Pouteau C., Dole P., Cathala B., Averous L. and Boquillon N., Polymer Degradation and Stability, 81, (2003), 9.

21. Rozman H. D., Tan K.W., Kumar R. N. And Abudakar A., Polymer International, 50, (2001), 561.

22. Thielemans W. and Wool R. P., Composites: Part A, 35, (2004), 327.

23. Karger-Kocsis J., Advanced Composites Letters, 2, (1998), 39.

24. Karger-Kocsis J, Harmia T. and Czigány T., Composites Science and Technology, 54, (1995), 287.

25. Benevolenski O.I. and Karger-Kocsis J, Composites Science and Technology, 61, (2001), 2413.

26. Karger-Kocsis J. and Czigány T., Polymers and Polymer Composites, 1, (1993), 329.

27. Romhány G., Czigány T. and Karger-Kocsis J., Composites Science and Technology (in press).

28. Karger-Kocsis J. and Czigány T., Composites: Part A, 29, (1998), 1319.

29. Karger-Kocsis J, Harmia T., Czigány T. and Mayer J., Plastics, Rubber and Composites Processing and Application, 25, (1996), 109.

Tables

Table 1.Tensile data for the PP and its jute cloth reinforced composites

Material	σ [MPa]	ε%	E-modulus[GPa]
PP	30.18 ± 0.58	13.9 ± 0.67	1.33 ± 0.09
PPJ	40.62 ± 0.46	5.32 ± 0.32	2.89 ± 0.01
PPGJ	40.93 ± 2.91	3.07 ± 0.12	3.97± 0.22
PPLJ	39.21 ± 0.66	3.42 ± 0.08	3.40 ± 0.10
PPJLa	34.59 ± 3.06	2.97 ± 0.39	3.38 ± 0.12

Table 2. Fracture mechanics parameters for PP/ jute cloth composites.

Material	K_Q [MPa $m^{1/2}$]	K_C [MPa $m^{1/2}$]
PPJ	6.58	5.72
PPJG	5.25	4.87
PPJL	5.06	4.92
PPJLa	6.82	6.59

Figure captions

Figure 1. Experimental set-up, including the dimensions of the SEN-T specimen, and the positioning the AE sensors.

Figure 2. Apparent stress-strain curves for jute cloth.

(——) jute 1 layer, (- - -) jute 3 layers.

Figure 3. Characteristic stress-strain curves for the PP/jute cloth composites.

(——) PPJ, (- - -) PPGJ, (·····) PPLJ, (- · - ·) PPJLa.

Figure 4. Typical cumulative AE events versus strain curves registered on tensile loaded dumbbells.

(——) PPJ, (- - -) PPGJ, (·····) PPLJ, (- · - ·) PPJLa, Jute 3 layers (– · –).

Figure 5. Fracture of dumbbell cut from PPLJ. (Notes: the fracture surface is on the left. The mesh size of the jute cloth can be seen).

Figure 6. a) Typical stress-strain curve for a dumbbell of PPLJ. b) AE amplitude distributions of PPJ, PPGJ and jute cloth (3 layers).

Figure 7. Tensile fracture surfaces of PPJ (back; multiple matrix cracking, long pull-out) and PPGJ (front; short pull-out).

Figure 8. Effects of interface modification on the load-displacement behaviour.

(——) PPJ, (- - -) PPGJ, (·····) PPLJ, (- · - -) PPJLa

Figure 9. 2D contour plots of the damage zone. Note: Located AE events were considered up to $F_{max.}$

Figure 10. Fracture surfaces of PPJ (a) and PPJLa (b) composites.

Figure 11. Fracture surfaces of PPGJ (a) and PPLJ (b) composites.

Figure 12. Fracture surface of PPLJ composite.

Figure 1

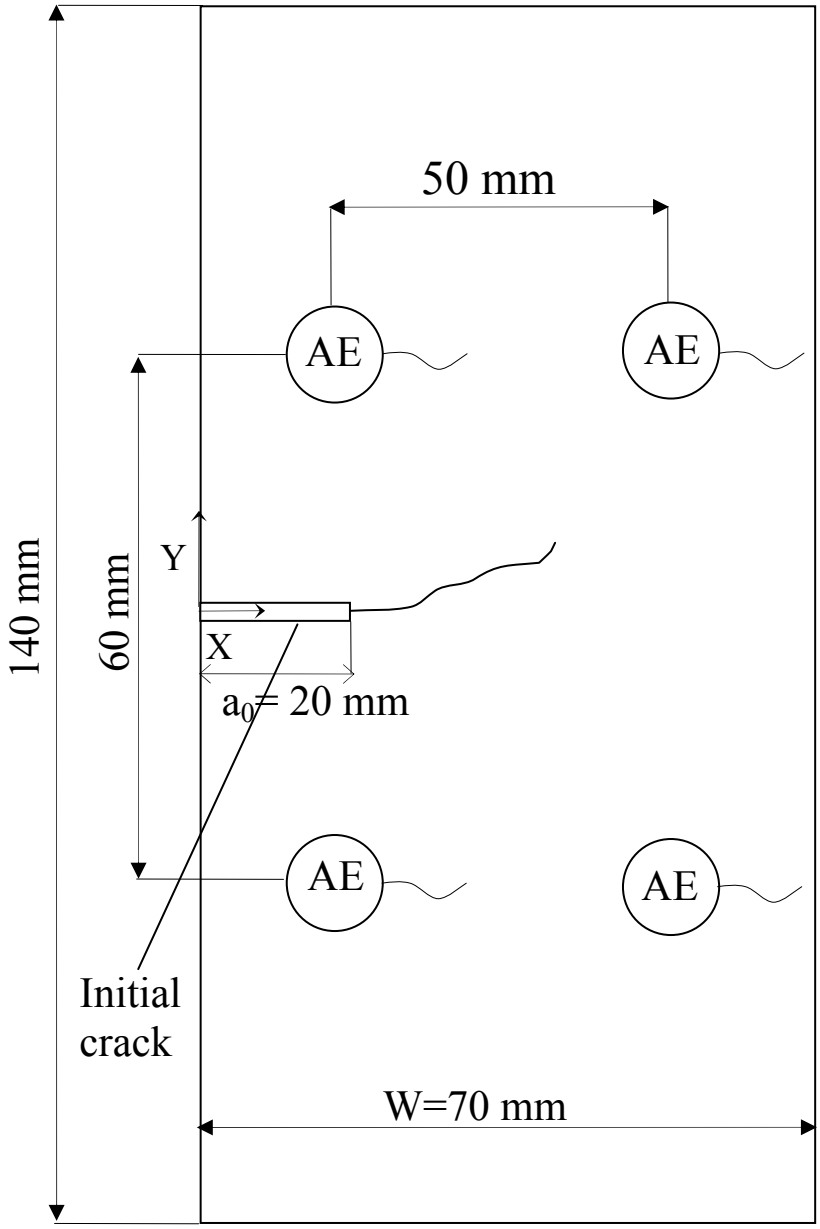

Figure 2

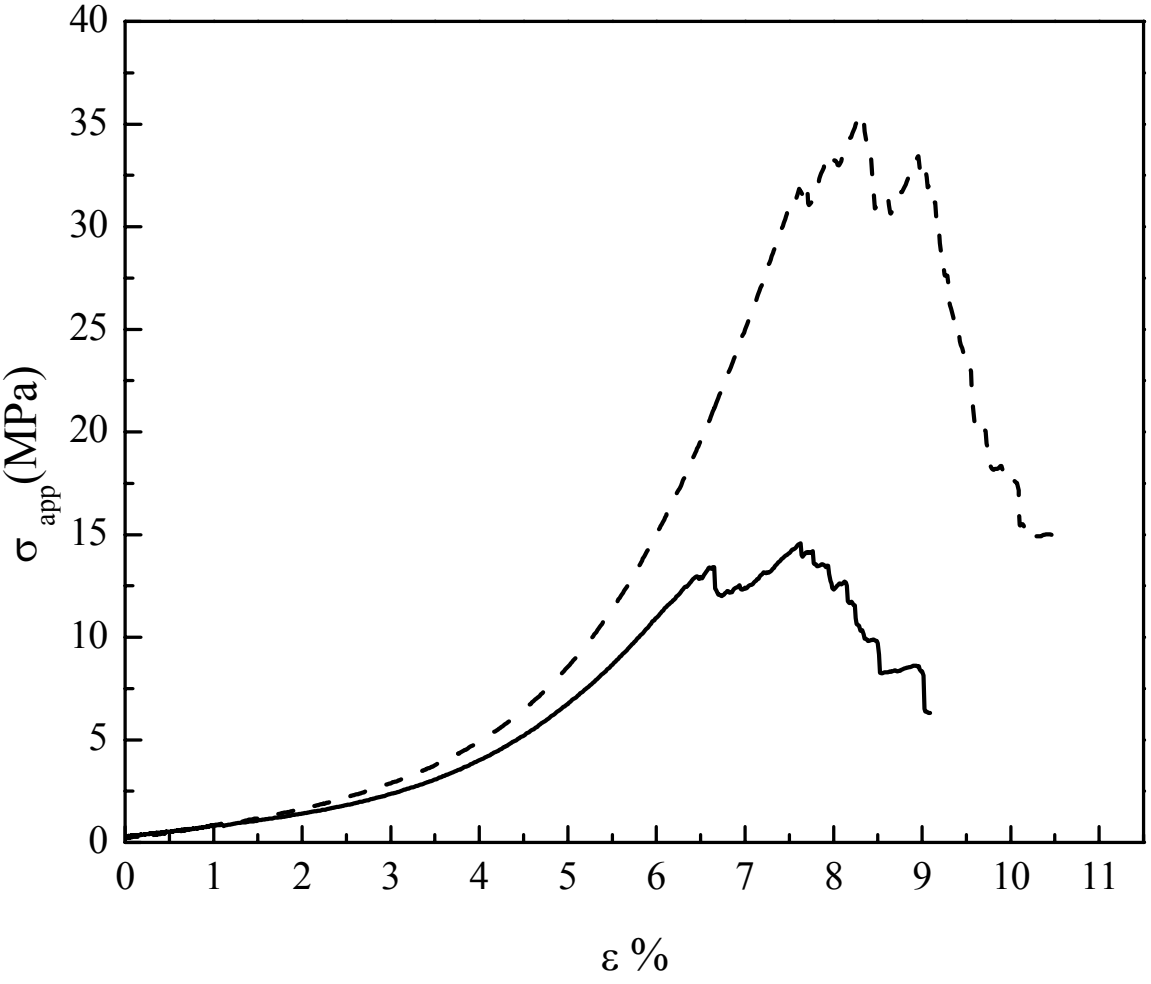

Figure 3

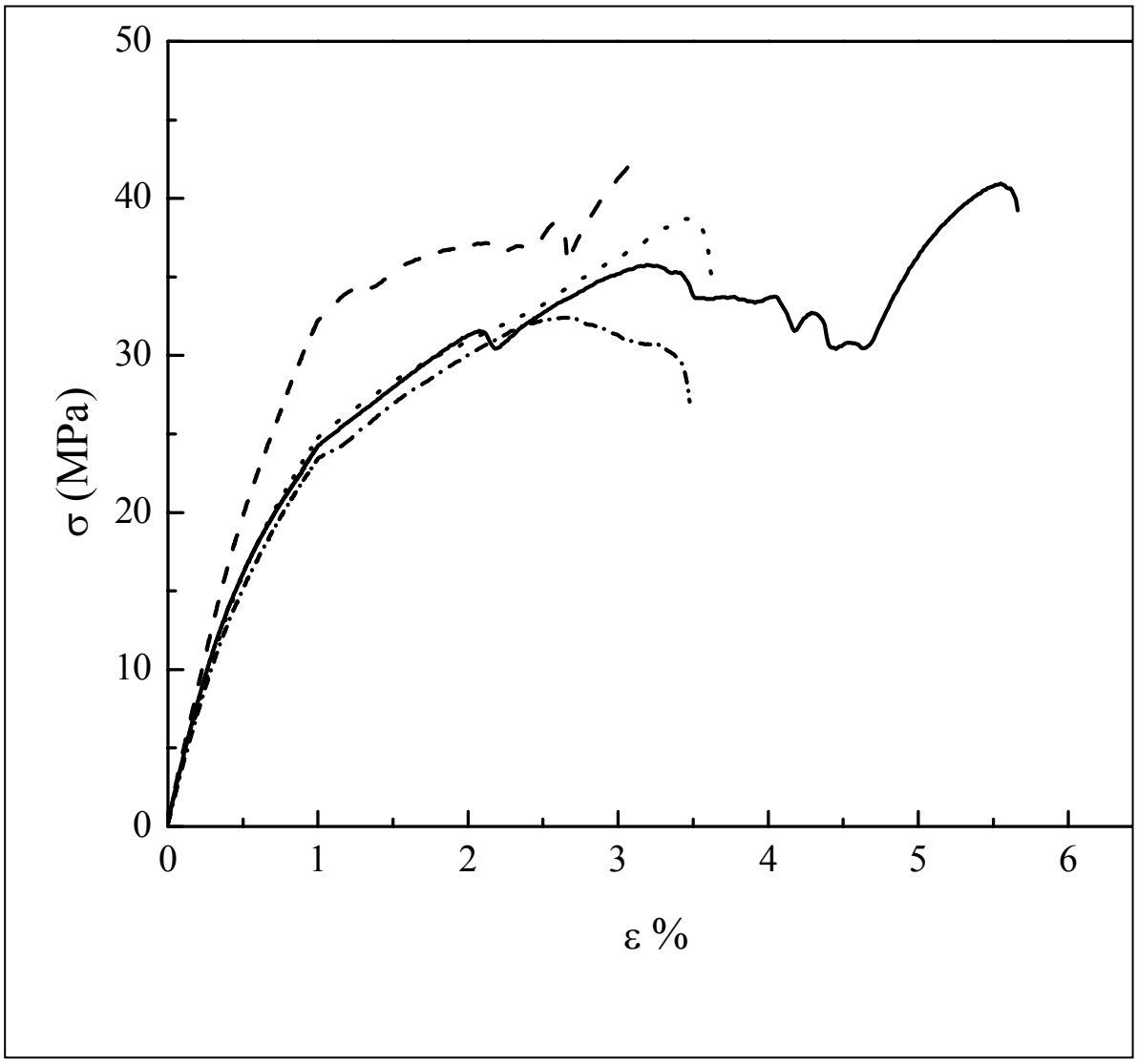

Figure 4

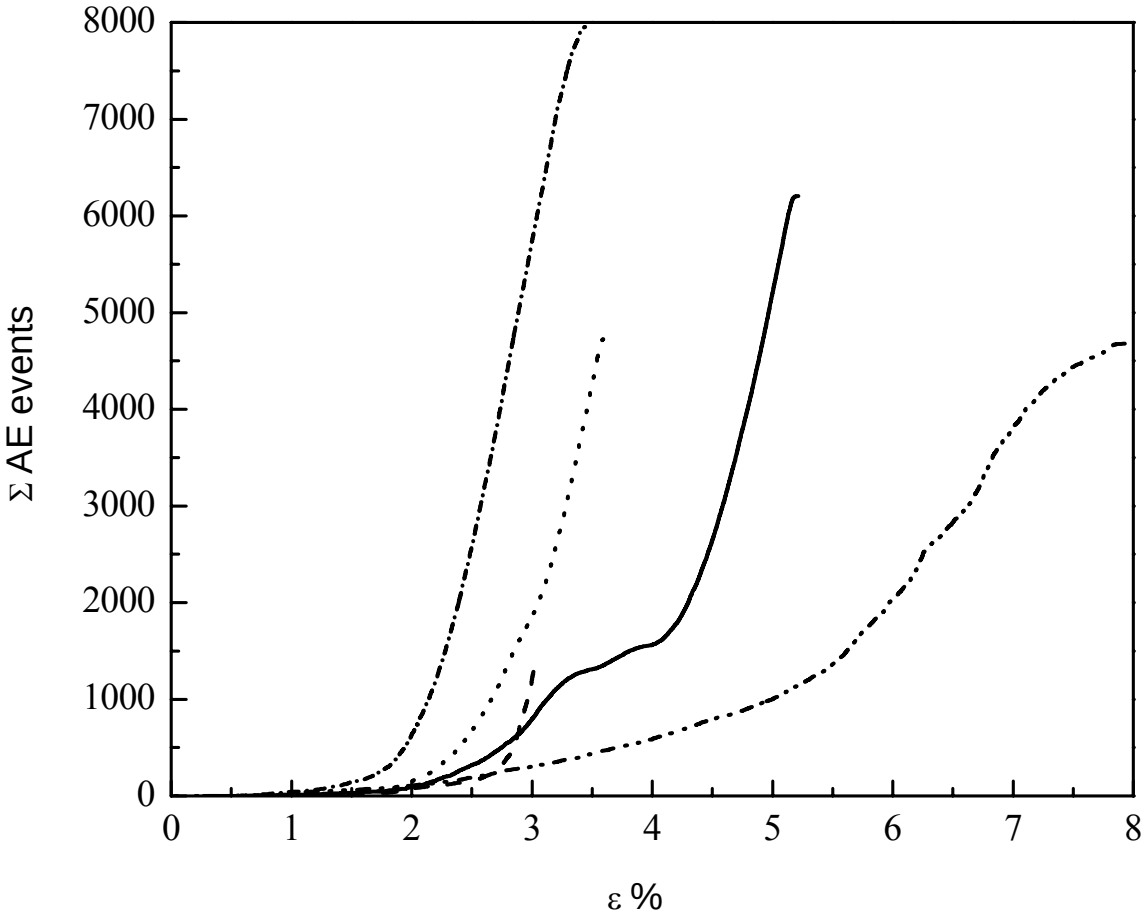
8000
7000
6000
5000
4000
3000
2000
1000
0
Σ AE events
0
1
2
3
4
5
6
7
8
ε %

Figure 5

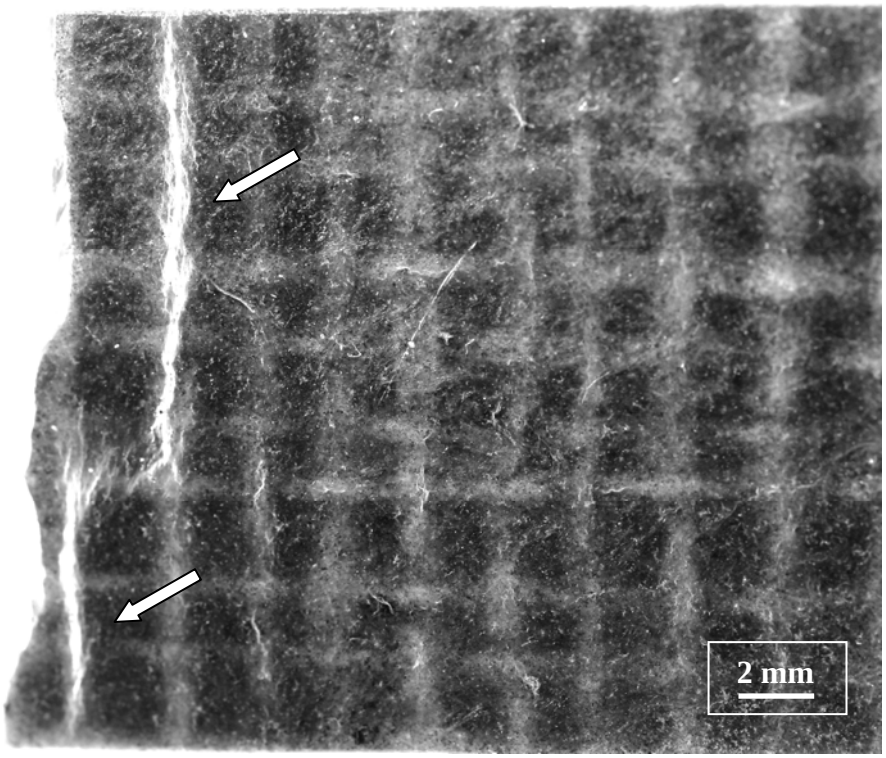

Figure 6 a)

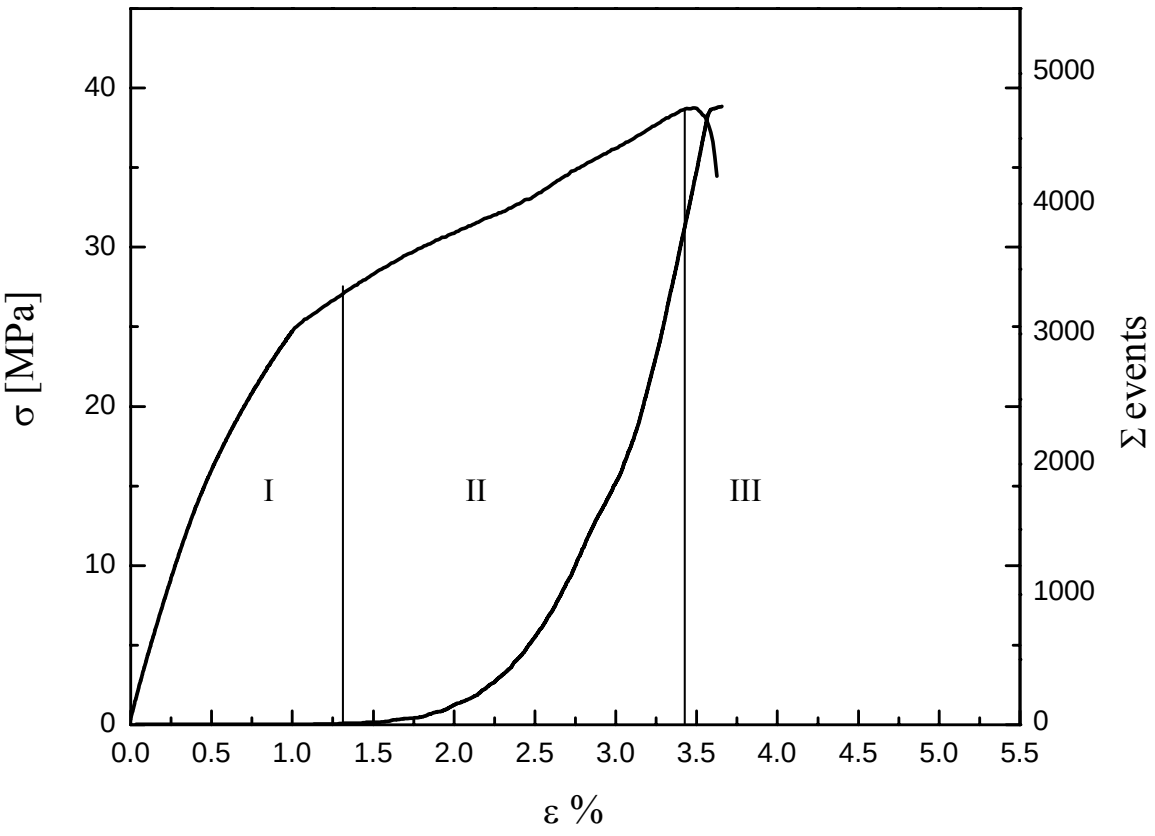
σ [MPa]
Σ events
ε %
I
II
III
0
10
20
30
40
0
1000
2000
3000
4000
5000
0.0
0.5
1.0
1.5
2.0
2.5
3.0
3.5
4.0
4.5
5.0
5.5

Figure 6 b)

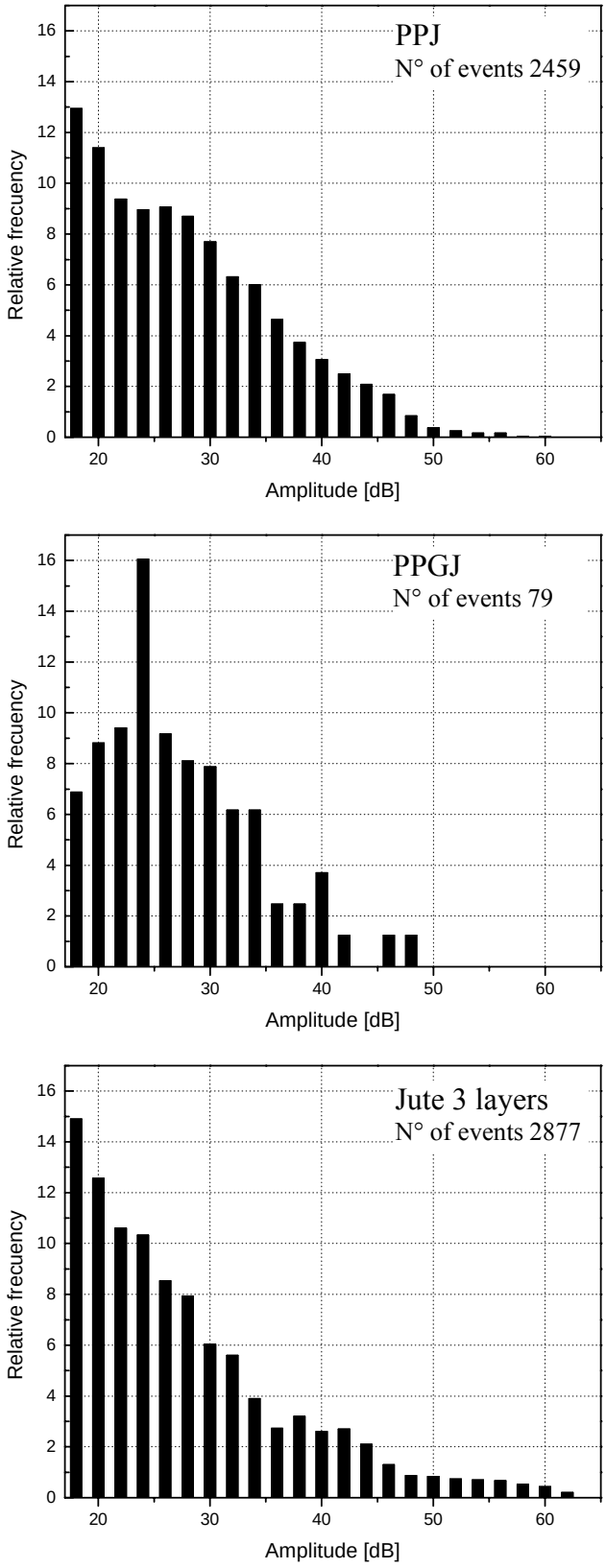
PPJ
N° of events 2459
PPGJ
N° of events 79
Jute 3 layers
N° of events 2877
Relative frecuency
Amplitude [dB]

Figure 7

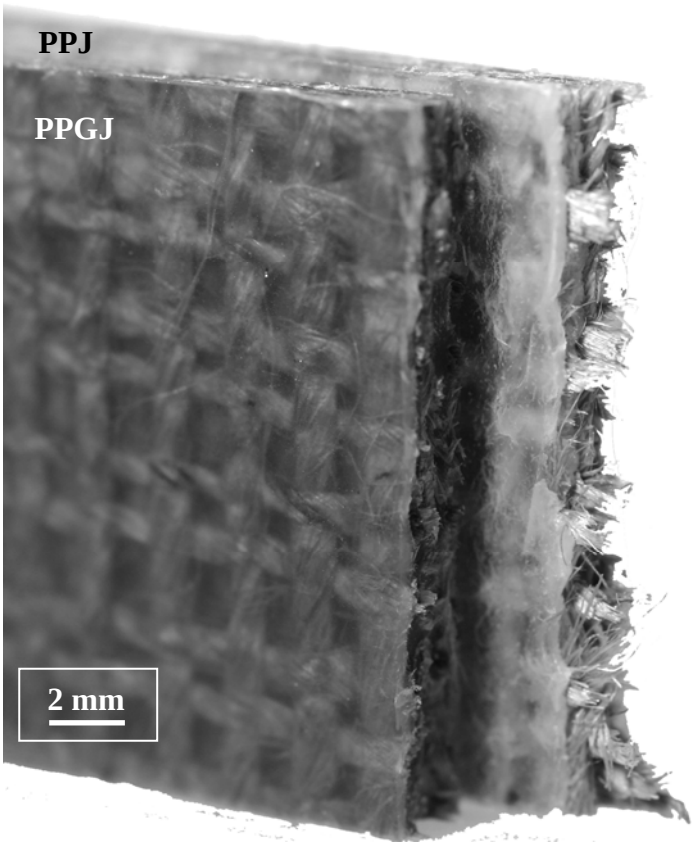

Figure 8

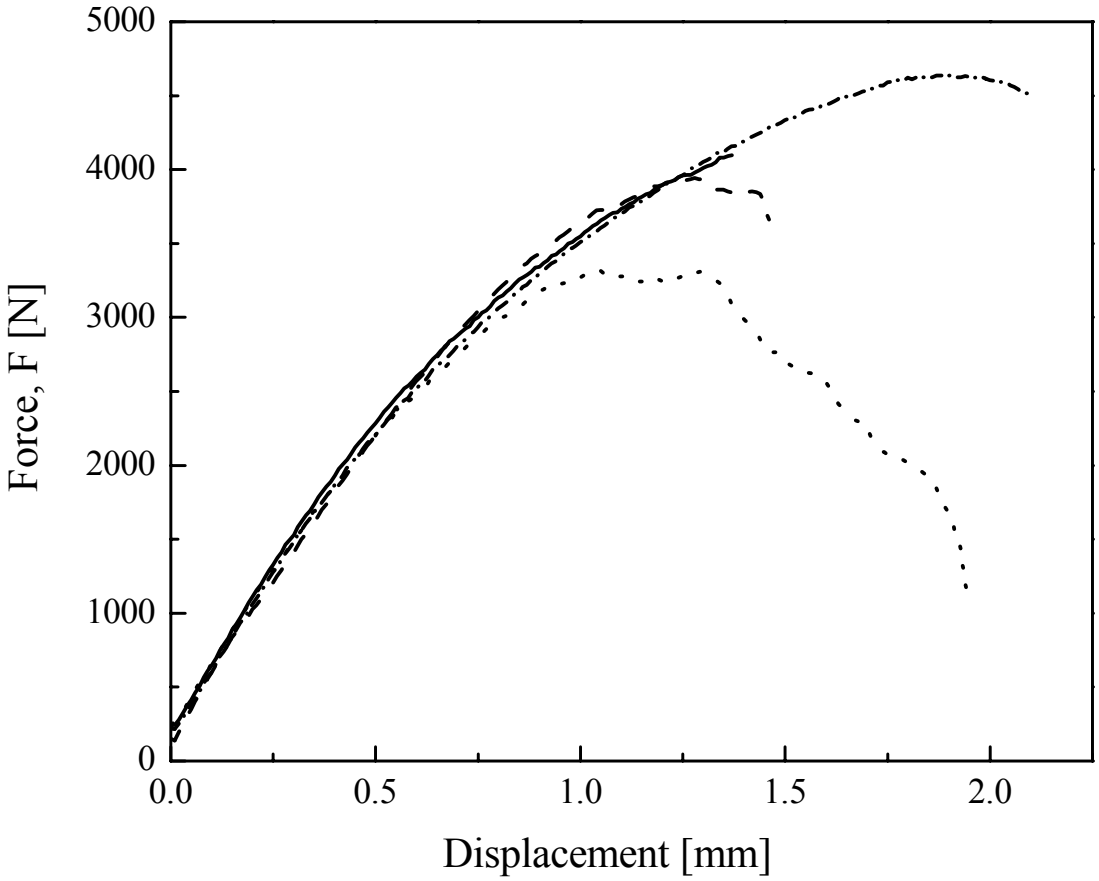
5000
4000
3000
2000
1000
0
Force, F [N]
0.0
0.5
1.0
1.5
2.0
Displacement [mm]

Figure 9.

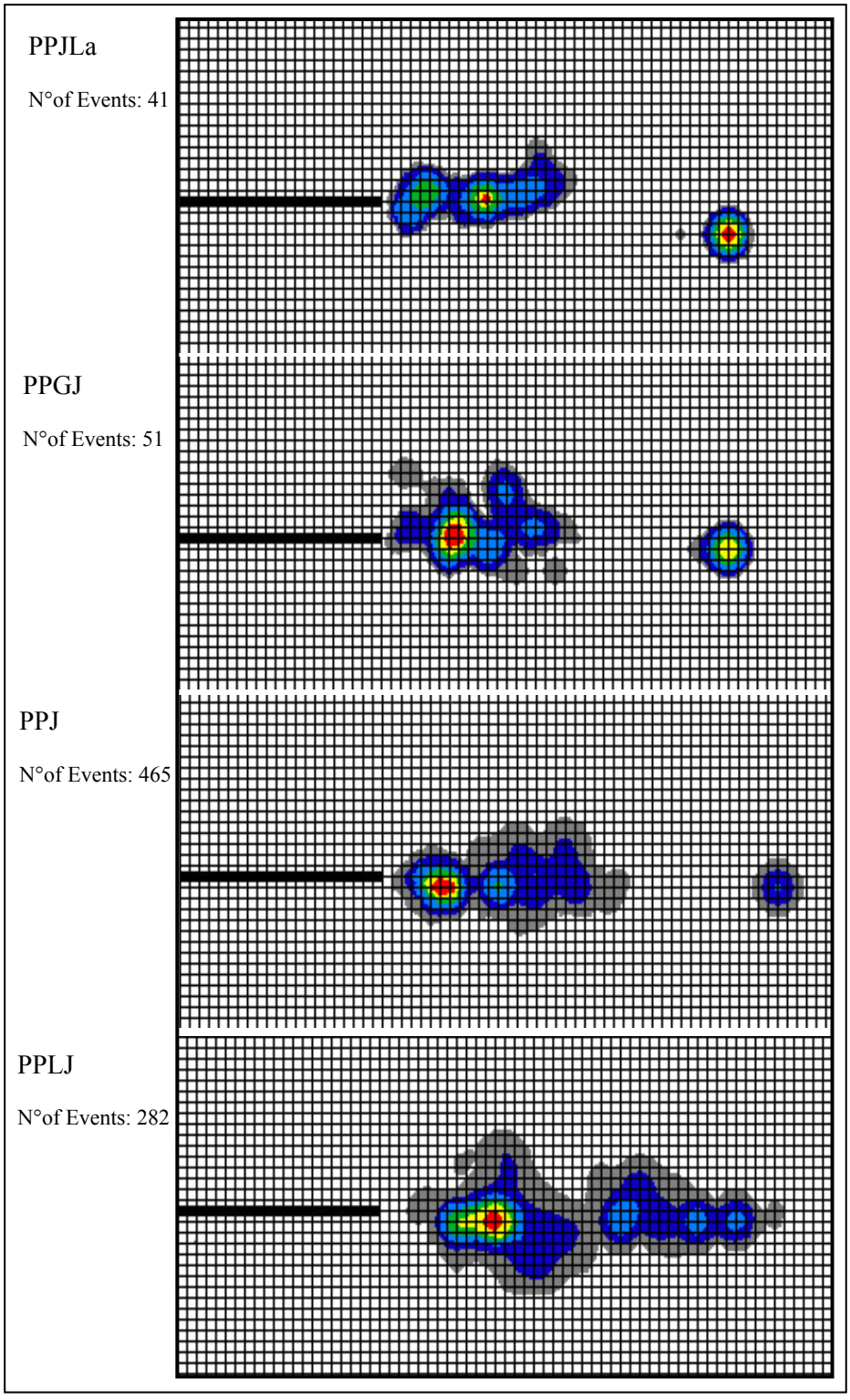
PPJLa
N°of Events: 41
PPGJ
N°of Events: 51
PPJ
N°of Events: 465
PPLJ
N°of Events: 282

Figure 10

a)

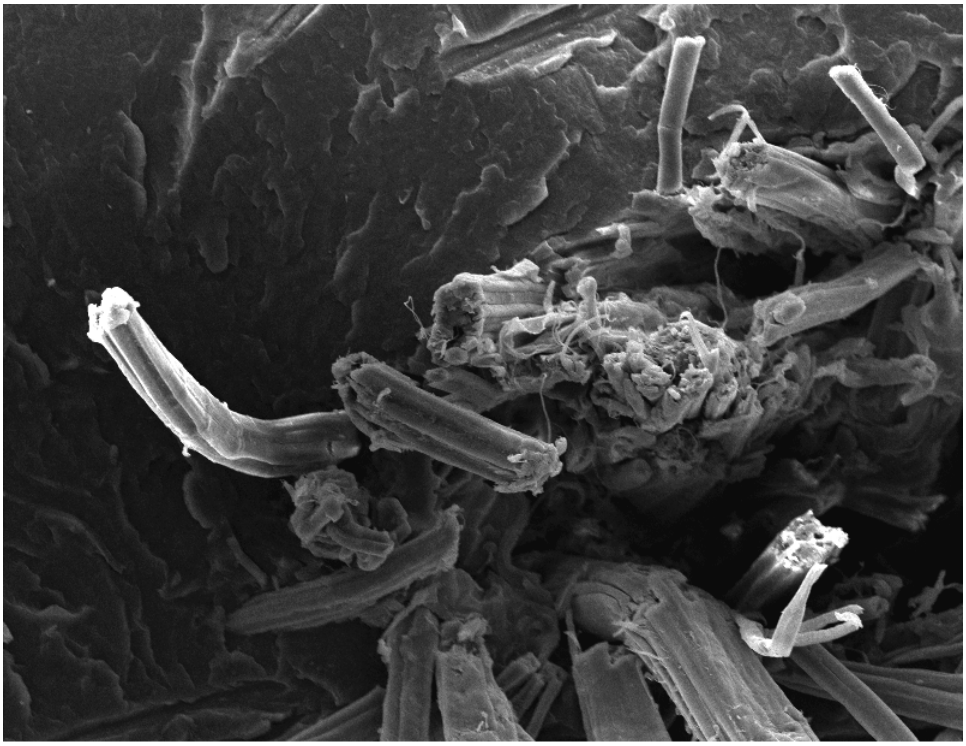

b)

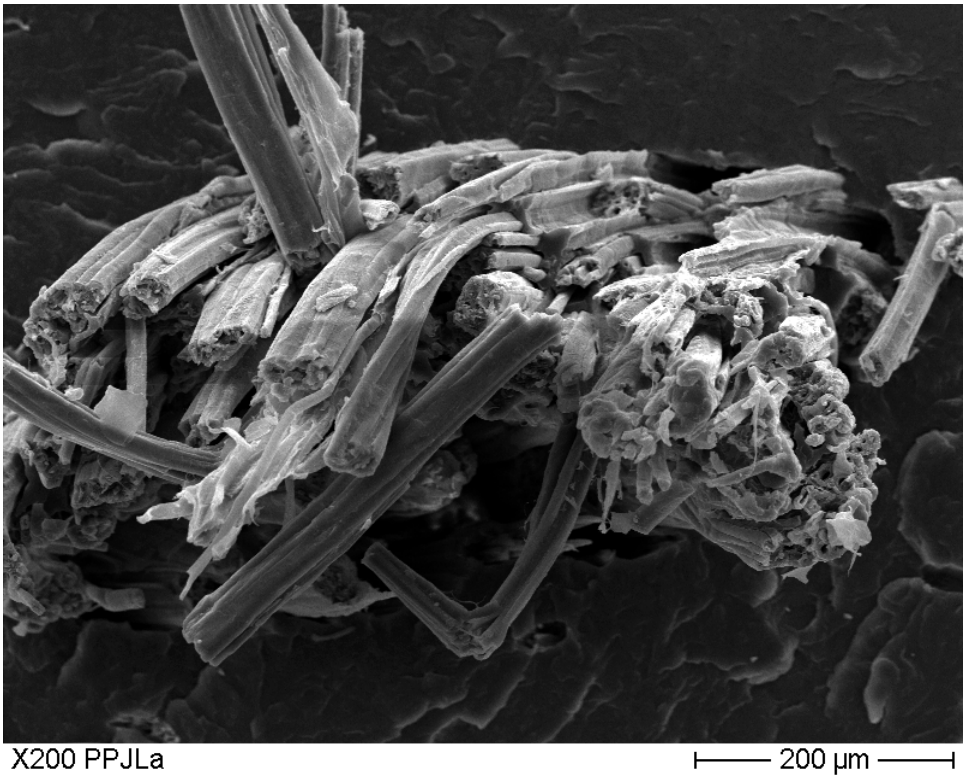

Figure 11

a)

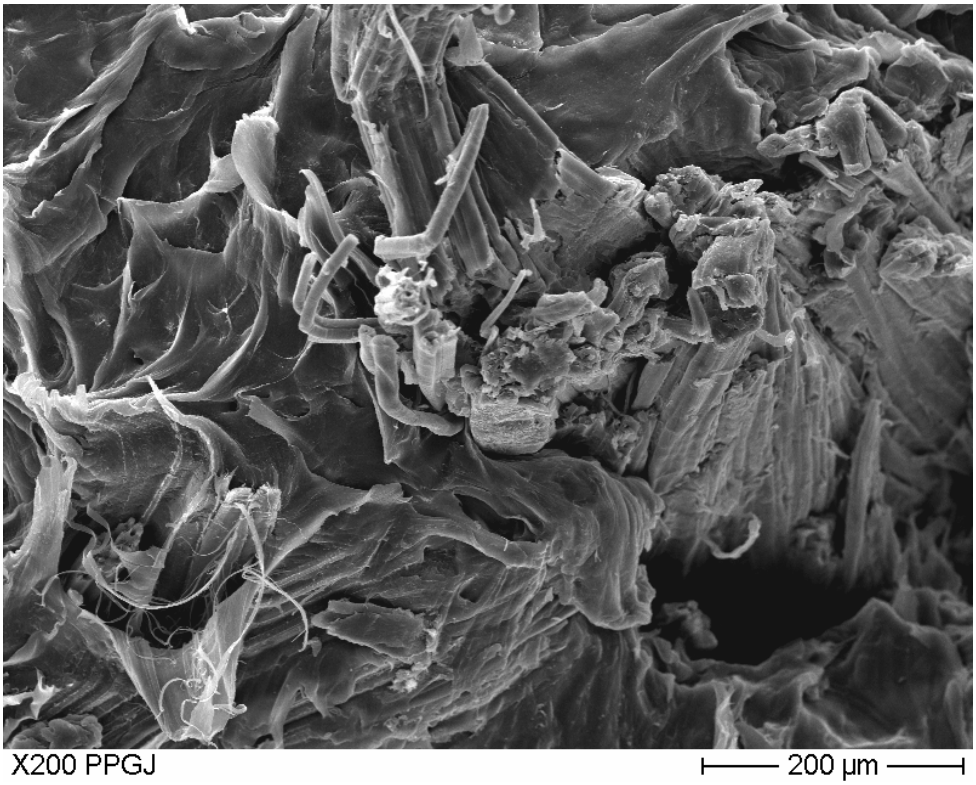

b)